Multi-objective Cooperative Optimization of Photovoltaic-driven Refrigerated Warehouse with Ice Storage

R. Ma
Southwest Forestry University– China
M. Li
Yunnan Normal University– China
H. Zhao
Southwest Forestry University– China
Yunnan Normal University– China

Introduction

Photovoltaic (PV)-driven cold storage is a promising solution for decarbonizing the energy-intensive cold chain [1,2]. However, solar intermittency causes dynamic mismatches among system components, leading to inefficient operation and poor stability [3]. Although ice storage can buffer cooling demand, the strong coupling between PV generation, refrigeration dynamics, and thermal storage requires coordinated control [4]. Conventional fixed-superheat strategies fail to adapt to real-time solar variations, resulting in low self-consumption and excessive temperature fluctuations [5]. This mismatch often forces the system to rely on grid backup or waste excess PV power, undermining both energy efficiency and economic viability. Furthermore, frequent compressor cycling under fluctuating conditions accelerates equipment wear and increases maintenance costs. To overcome these limitations, adaptive control strategies that respond to both solar availability and storage status are urgently needed. To address this, we propose a multi-objective cooperative optimization framework that simultaneously improves energy efficiency, economic performance, and temperature stability in PV-driven refrigerated warehouses with ice storage.

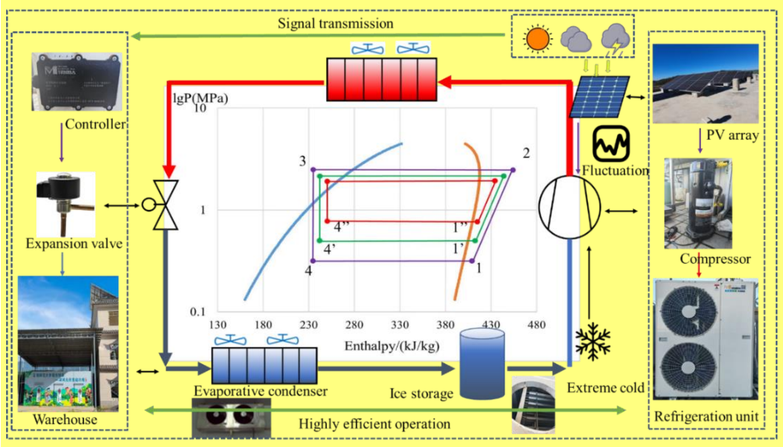

Fig. 1. System operation principle of the PV-driven refrigerated warehouse with ice storage.

Construction of the system

As shown in Fig. 1, to more fully utilize the cooling capacity of the refrigeration cycle, we have added an ice storage tank after the surface cooler. This improvement stems from observations made during experiments: as the temperature inside the storage room decreases, it becomes increasingly difficult for the refrigerant to fully evaporate within the surface cooler of the refrigerated warehouse. Liquid refrigerant that has not evaporated is carried out of the surface cooler and continues to evaporate at the gas-liquid separator, leading to significant frost accumulation on the gas-liquid separator, which in turn results in partial wastage of the system's cooling capacity.

Therefore, we have connected an ice storage tank in series after the surface cooler, allowing the partially evaporated refrigerant to complete its evaporation process within the ice storage tank. This approach avoids energy loss due to premature evaporation and excessive frosting on the gas-liquid separator. By fully utilizing the latent heat of the refrigerant for ice formation, the system simultaneously satisfies cooling load requirements while storing thermal energy for later use. Not only does this enhance the system's effective performance, but it also increases the operational efficiency and economic viability of the entire refrigeration system.

Results

Fig. 2 shows that, at fixed irradiance, evaporation pressure rises with expansion valve opening—e.g., by 130% (1.3→2.5 bar) when opening increases from 20% to 25% at 750 W/m²—but the sensitivity diminishes at higher openings due to increased evaporator load. This diminishing sensitivity suggests that the evaporator approaches its maximum heat absorption capacity, beyond which further valve opening yields only marginal pressure gains. The practical implication is that valve adjustments must be carefully balanced to avoid overshooting the optimal operating point, which could lead to compressor overload or reduced system COP. Evaporation pressure is more responsive than condensation pressure to changes in both irradiance and valve opening, owing to the evaporator's smaller thermal capacity and R507a's subcritical phase-change behavior. The higher responsiveness of evaporation pressure also means that transient fluctuations in solar irradiance can directly destabilize the evaporation process, necessitating fast-acting control strategies to maintain stable superheat. Experimental evaporation pressures agree well with theoretical values (RMSE = 0.274 at 750 W/m²). This good agreement validates the accuracy of the thermodynamic model and confirms that the observed pressure responses are physically consistent, providing confidence for using the model in subsequent control system design.

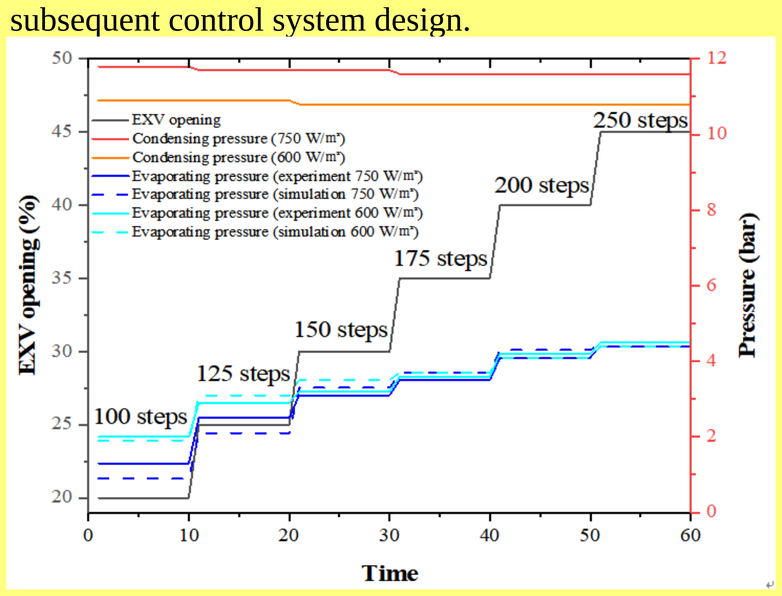

Fig. 2. Expansion valve effects on pressures under varying irradiance.

Fig. 3shows that, at a fixed expansion valve opening, evaporation temperature drops as irradiance rises—e.g., by ~9 °C per 100 W/m² at 20% opening, but only 1.4 °C at 60% opening—due to higher compressor speed lowering evaporator pressure (and thus temperature via the refrigerant's pressure–temperature relationship). Conversely, increasing valve opening raises evaporation temperature more dramatically under high irradiance (from −45 °C to 21 °C at 500 W/m²) than under low irradiance (22 °C to 27 °C at 200 W/m²). Critically, at 20% opening and irradiance >650 W/m², evaporation pressure falls below 0.1 MPa, risking gas locking and system failure. Hence, irradiance-adaptive valve control is essential for safe, efficient operation.

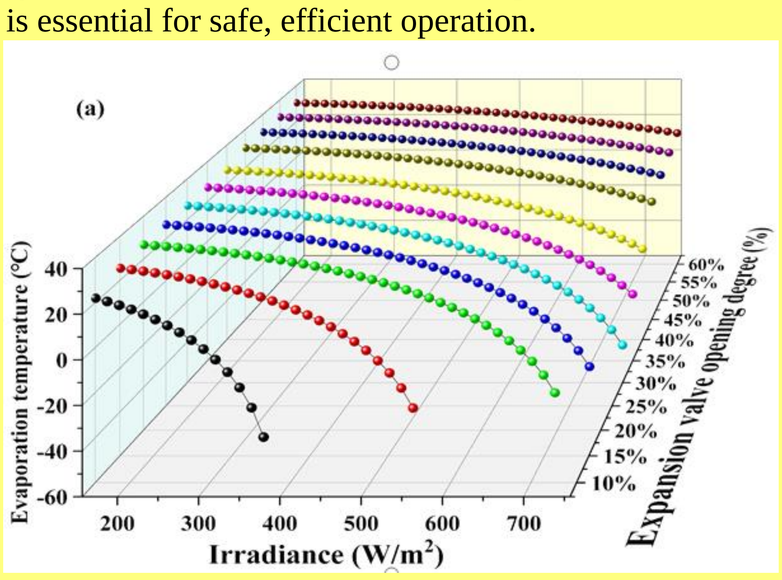

Fig. 3. Variation of evaporation temperature with expansion valve opening under different irradiance levels.

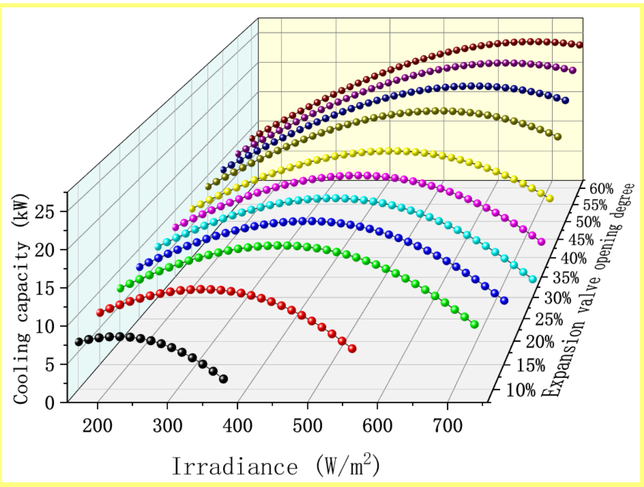

Fig. 4. Variation of cooling capacity with expansion valve opening under different irradiance levels.

The Fig. 4 shows the effect of expansion valve opening on the system's cooling capacity at different solar irradiances. At this time, the condensing pressure is 1.4 MPa, the condensing temperature is approximately 28°C, the subcooling degree is 2°C, and the superheating degree is 5°C. As shown in the figure, the cooling capacity generally increases and then decreases with increasing irradiance at a certain valve opening. This is primarily due to the increase in irradiance leading to an increase in compressor speed, which causes more refrigerant to be delivered to the evaporator, thus increasing the cooling capacity. However, as the compressor speed continues to increase, the refrigerant gas is compressed more quickly, leading to a further decrease in pressure and temperature within the evaporator. This results in a further reduction in the refrigerant density within the evaporator, causing a decrease in the refrigerant mass flow rate through the evaporator, and ultimately leading to a decrease in cooling capacity. The above results indicate that adjusting the expansion valve opening based on changes in irradiance can optimize the cooling capacity of the system.

Conclusions

This study presents a multi-objective optimization framework for photovoltaic-driven cold storage with ice storage, significantly improving performance over conventional control: daily COP increases by 22.7%, PV self-consumption reaches 90.3%, temperature fluctuation stays within ±0.5°C, and operating costs drop by 20.5%. The approach offers practical guidance for efficient, stable, and cost-effective renewable-powered cold chain systems.

References

[1] Journals Shi J, Han D, Li Z, et al. Electrocaloric cooling materials and devices for zero-global-warming-potential, high-efficiency refrigeration. Joule 3(5), 1200-1025 (2019).
[2] Journals Nastasi B, Mazzoni S, Groppi D, et al. Solar power-to-gas application to an island energy system. Renewable Energy 164, 1005-1016 (2021).
[3] Journals Ibrahim N I, Yahiaoui A, Garkuwa J A, et al. Solar cooling with absorption chillers, thermal energy storage, and control strategies: A review. Journal of Energy Storage, 97, 112762 (2024).
[4] Journals Rabaia M K H, Abdelkareem M A, Sayed E T, et al. Environmental impacts of solar energy systems: A review. Science of The Total Environment, 754, 141989 (2021).
[5] Journals Li G, Han Y, Li M, et al. Study on matching characteristics of photovoltaic disturbance and refrigeration compressor in solar photovoltaic direct-drive air conditioning system. Renewable Energy, 172, 1145-1153 (2021).